Materials Letters 319 (2022) 132271

Contents lists available at ScienceDirect

Materials Letters

journal homepage: www.elsevier.com/locate/matlet

$SrTiO_3/Ag_2O$ embedded in N-doped carbon nanocomposite for advanced photocatalytic degradation of dichlorodiphenyltrichloroethane (DDT)

Norah Alhokbany, Tansir Ahamad *, Jahangeer Ahmed *, Saad M Alshehri

Department of Chemistry, King Saud University, Riyadh 11451, Saudi Arabia

ARTICLE INFO

Keywords:
Nanocomposites
Carbon materials
Elecctron microscopy
Photocatalysis

ABSTRACT

For environmental remediation, a novel $SrTiO_3/Ag_2O$ heterostructure embedded in N-doped carbon (NDC) nanocomposite has been fabricated by the polymeric precursor method. The prepared $SrTiO_3/Ag_2O$-NDC nanocomposite has been used as a photocatalyst in dichlorodiphenyltrichloroethane (DDT) degradation reactions. The results showed that the tuned bandgap increased the photocatalyst's catalytic efficiency, and about 94.2% of the DDT degraded within 180 min. The role of the photo-generated spices was also determined using radical scavenging experiments and ESR spectra. The results showed that h^+ and $OH^{\bullet-}$ play prominent roles in DDT degradation under visible light. The intermediate and the degradation mechanism were determined using GC–MS and DFT calculations. The reusability and excellent catalytic efficiency of the $SrTiO_3/Ag_2O$-NDC photocatalyst show its strengths in breaking down of organic pollutants.

1. Introduction

The use of organochlorine pesticides such as dichlorodiphenyltrichloroethane (DDT) for insect control in crops, gardens, and household is due to their long-lasting effectiveness and low cost. Its highly toxic, resistant to degradation, and a tendency to bio-accumulate, diminishing its benefits. In addition, studies show a range of human health effects related to DDT, including breast cancers, male infertility, miscarriages, and damage to the nervous system and liver [1]. Therefore, it is imperative to develop effective techniques to remediate DDT-contaminated soil and water. Advanced photocatalytic degradation has been used extensively to remove organic pollutants from contaminated water [2–3]. Therefore, producing the efficient photocatalysts at a low cost, excellent catalytic efficiency, and stability under visible light is essential. $SrTiO_3$ photocatalyst has a wild bandgap of ~ 3.2 eV, which requires high-energy UV radiation and consumes around less than 10% of solar energy. The bandgap of the photocatalyst can be tuned by employing elemental doping or combining two semiconductors and developing more efficient nanocomposites for visible-light-driven photo-catalysis [4]. Ag_2O is a typical p-semiconductor with a bandgap of ~ 1.2 eV, has been used as an efficient photocatalyst in wastewater treatment due to its excellent absorption capacity in visible light [5]. $Ag_2O/PbBiO_2Br$ heterostrucrures were reported as the efficient photocatalysts for dye degradation reactions under visible-light irradiation [6]. The development of an efficient photocatalyst for the photo-degradation of organic pollutants should absorb the full range of sunlight and charge separation. In addition, according to the previous study, it was found that the adsorption of the organic pollutants over the catalytic system increases the catalytic efficiency, and N-doped graphitic carbon is suitable for the adsorption of the DDT and charge transfer in the catalytic system. Present study focuses on the synthesis of $SrTiO_3/Ag_2O$ heterostructure embedded in N-doped carbon as an efficient photocatalyst in the degradation of DDT for environmental remediation.

2. Synthesis of the photocatalysts

To produce the $SrTiO_3/Ag_2O$-NDC, 3 gm of urea–formaldehyde pre-polymer was dissolved in THF and mixed with 5.68 g (0.20 mol) of titanium isopropoxide. Then 4.23 g (0.20 mol) of strontium nitrate and 0.339 g (0.020 mol) of $AgNO_3$ were added dropwise. The mixture was heated at 75 °C for 3 h to make the brown color polymer metals complex. The obtained complex was re-precipitated with methanol and washed with water. The resulting product was then transferred to a Teflon-lined stainless-steel autoclave and heated to 150 °C for 24 h. The resulting product was washed several times with deionized water and further calcined at 800 °C for 8 h under helium flow. Finally, the $SrTiO_3/Ag_2O$-NDC nanocomposites were washed with dil HNO_3, deionized water, and then dried in a vacuum oven. The molar proportion of Ag_2O has been

* Corresponding authors.
E-mail addresses: tahamed@ksu.edu.sa (T. Ahamad), jahmed@ksu.edu.sa (J. Ahmed).

https://doi.org/10.1016/j.matlet.2022.132271
Received 1 March 2022; Received in revised form 27 March 2022; Accepted 12 April 2022
Available online 15 April 2022

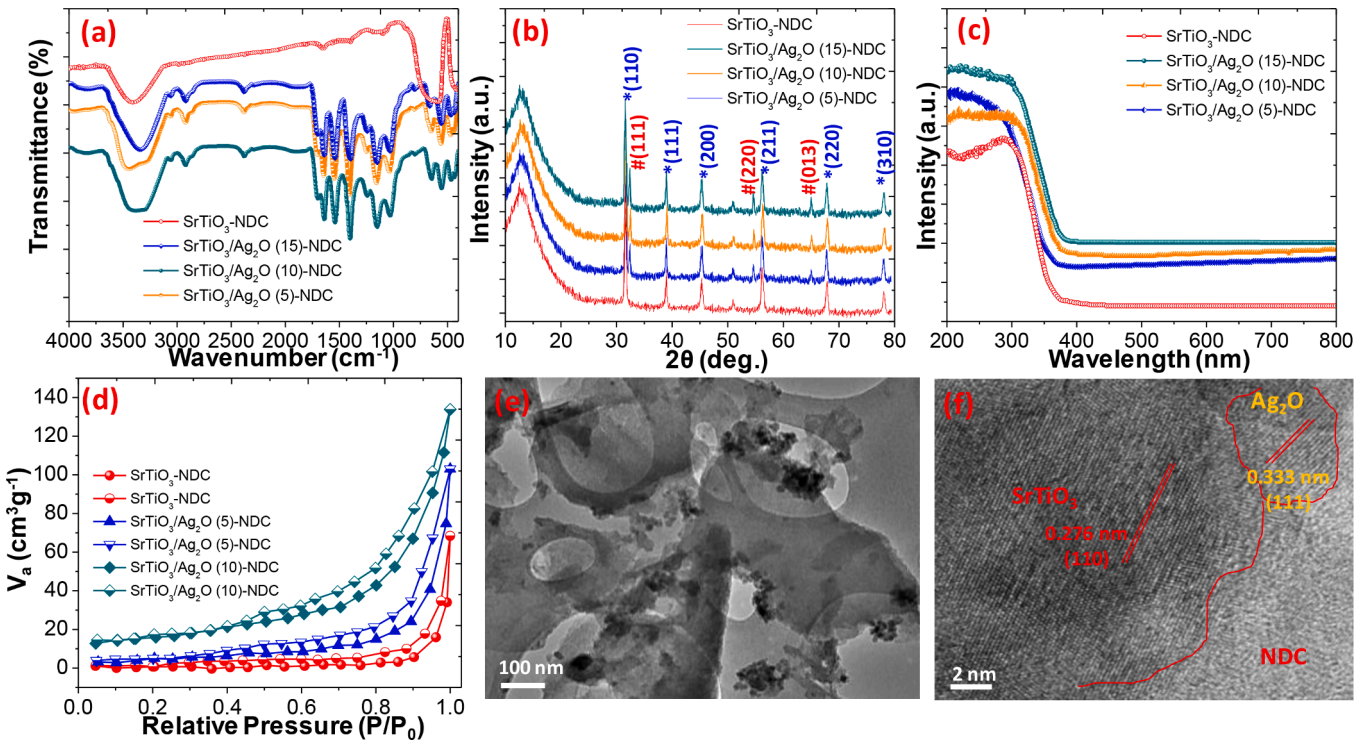

Fig. 1. (a) FTIR spectra (b) XRD spectra (c) DRS Spectra (e) N_2 adsorption desorption isotherm (e) TEM and (f) HRTEM of $SrTiO_3/Ag_2O$-NDC based nanocomposites.

changed with 5, 10 and 15 mol% to the $SrTiO_3$ and labeled as $SrTiO_3/Ag_2O$(5)-NDC, $SrTiO_3/Ag_2O$(10)-NDC, and $SrTiO_3/Ag_2O$(15)-NDC using a similar procedure as discussed above.

3. Results and discussion

The synthetic route for the fabrication of $SrTiO_3/Ag_2O$-NDC is shown in supporting Figure SF-1. FTIR spectra of the nanocomposites show several bands and support the presence of pure $SrTiO_3$, Ag_2O nanoparticles in the N-doped carbon matrix (Fig. 1a). The crystalline nature and phase purity of $SrTiO_3$, Ag_2O nanoparticles were confirmed by XRD analysis. As shown in Fig. 1(b), several XRD peaks at $2\theta = 31.98$, 39.09, 46.49, 54.64, 57.81, 67.86, and 77.17 assigned to (1 1 0), (1 1 1), (2 0 0), (1 0 1), (2 1 1),(2 2 0) and (3 1 0) plane for perovskite $SrTiO_3$ (JCPDS no. 79–0176), while, other peaks at $2\theta = 33.1°$, 54.75° and 66.74° and assigned to (1 1 1), (2 2 0) and (0 1 3) planes of cubic phase of Ag_2O respectively (JCPDs Card No. 41–1104). Another broad peak assigned (0 0 2) plane of graphite carbon. No peak related to any

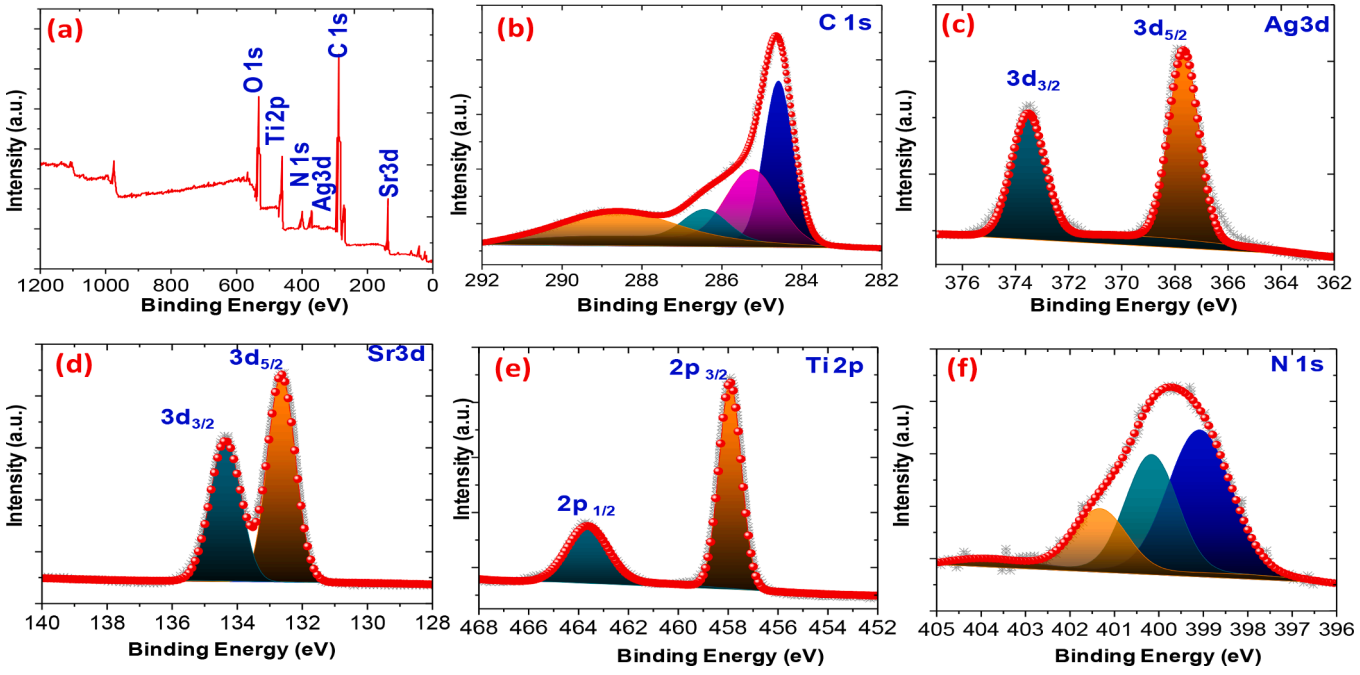

Fig. 2. (a) Wide XPS (b) C1s(c) Ag3d (e) Sr3d(e) Ti2p and (f) N1s of $SrTiO_3/Ag_2O$(10)-NDC nanocomposites.

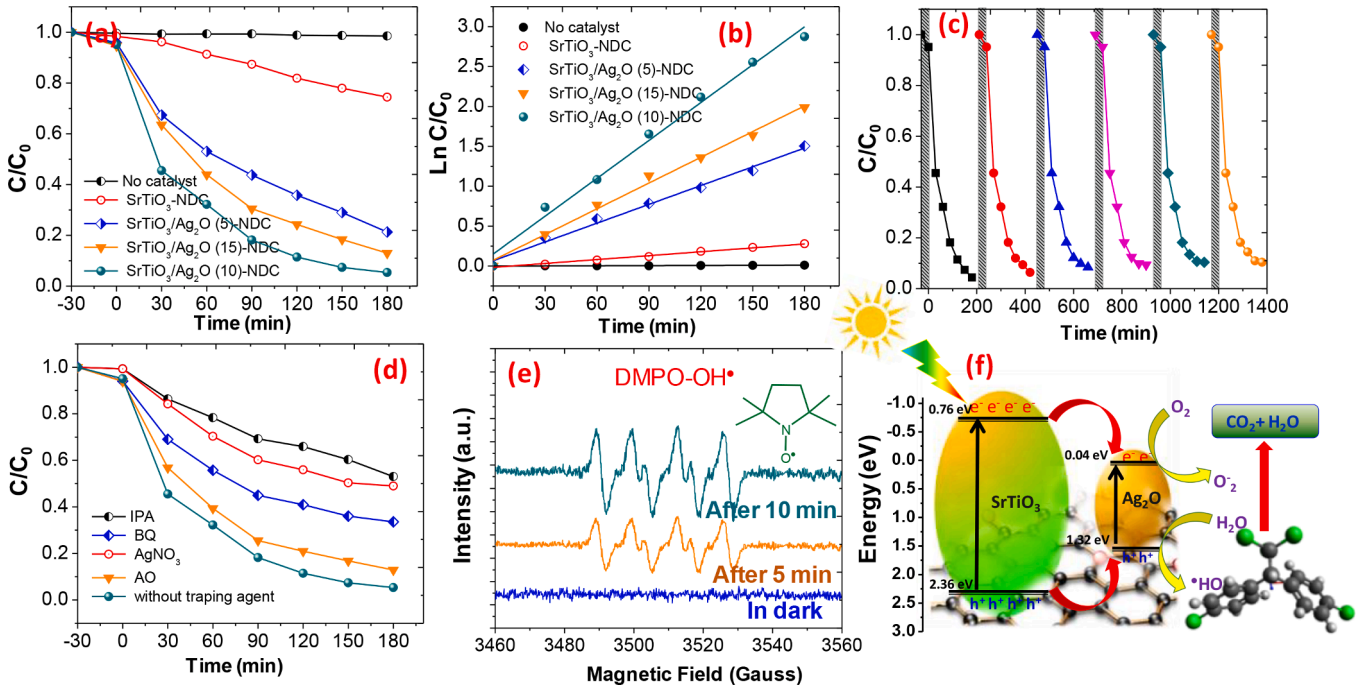

Fig. 3. (a) Effect of catalysts (b) photodegradation kinetics (c) reusability (d) effect of trapping agents (e) ESR spectral and (f) schematic band structure and charge-transfer process during the degradation of DDT.

impurity or unreacted metal was observed.

The DRS data of the nanocomposite was recorded in the range of 200–800 nm and illustrated in Fig. 1(c). It was found that the peak position was shifted towards the higher wavelength (red-shift) after the doping of Ag_2O. The bandgap was calculated and found to be 2.84 eV, which indicates that the bandgap energy is reduced after the doping of Ag_2O nanoparticles in the case of $SrTiO_3/Ag_2O$(10)-NDC, which helps to improve the photocatalytic efficiency. Fig. 1(d) shows the porosity and the surface area of the nanocomposite and determine using N_2 adsorption and desorption. The BET surface area and pore size were found to be 142.12 m^2/g 175.23 m^2/g and 247.32 m^2/g for $SrTiO_3/Ag_2O$(5)-NDC, $SrTiO_3/Ag_2O$(15)-NDC, and $SrTiO_3/Ag_2O$(10) –NDC. The morphology of the nanocomposite was examined using SEM and TEM images. As shown in Fig. 1(e), the TEM image shows the cubic structure of $SrTiO_3$ nanoparticles with a size range of 20–30 nm, while the Ag_2O nanoparticles were attached on the surface of $SrTiO_3$ with a size range of 10–25 nm. Both the nanoparticles were embedded into the carbon matrix. The HRTEM image, as shown in Fig. 1(f), show similar results to TEM, and both the nanoparticles were embedded into the NDC. HRTEM image of the $SrTiO_3/Ag_2O$(10)-NDC shows the fringes with interplanar spacings of 0.275 nm and 0.333 nm, is in good agreement with the (1 1 0) of $SrTiO_3$ and the (1 1 1) of Ag_2O, respectively.

The elemental composition and the state of the metal ions were determined using XPS, as shown in Fig. 2(a). Six XPS peaks were noticed and support that $SrTiO_3/Ag_2O$(10)-NDC contains Sr, Ti, Ag, O, N, and C elements. Fig. 2(b) shows a high-resolution spectrum of C 1s and demonstrates that four peaks were observed at 287.6. 286.48, 285.24, and 284.53 eV corresponding to C—N, C—O, O—C═O, and C—C/C═C, respectively [7]. The Ag 2p XPS spectrum, as shown in Fig. 2(c), deconvoluted into two peaks at 368.20 and 374.21 eV corresponding to Ag $3d_{5/2}$ and Ag $3d_{3/2}$, which supports the presence of Ag^+ as Ag_2O, which agrees with the XRD results. As shown in Fig. 2(d), the XPS peak of Sr3d was fitted into two peaks at 132.64 and 134.22 eV, which were assigned to $Sr3d_{5/2}$ and $Sr3d_{3/2}$, respectively. The deconvoluted Ti2p spectrum (Fig. 2e) shows two peaks at 457.98 and 463.89 eV and is assigned to $Ti2p_{3/2}$ and $Ti2p_{1/2}$, respectively. The N 1s spectrum consists of 399.40 eV, 400.18 eV, and 402.36 eV assigned to pyridinic-N, pyrrolic-N, and Oxidized-N, respectively. The O 1s spectrum shows four peaks at 529.97, 531.4, 531.7, and 533.3 due to lattice oxygen in $SrTiO_3$, Ag_2O, C═O, and C—O, respectively shown in supporting figure SF-2.

3.1. Photocatalytic assay

The catalytic activity of $SrTiO_3/Ag_2O$-NDC for the degradation of DDT under visible light is illustrated in Fig. 3(a). It was noticed that no degradation was observed without catalyst while in the presence of $SrTiO_3/Ag_2O$(10)-NDC, about to 94.2 % DDT degradation was found at room temperature and neutral pH [8]. The degradation kinetics revealed that the degradation was carried out using a first-order reaction, and the rate constant was found to be 0.015 min^{-1}, as shown in Fig. 3(b). The reusability is an important parameter for large-scale application and the catalyst so excellent reusability and after six cycles so 90.21 % degradation of DDT as shown in Fig. 3(c).

To determine the role of the reactive species, the radical trapping experiments were carried out in the presence of IPA, BQ, $AgNO_3$, and AO as a scavenger of $^{\bullet}OH$, $^{\bullet}O_2^-$, e-, and h^+ respectively [9]. It was noticed that no significant change was observed in the presence of BQ and $AgNO_3$, while in the presence of IPA and AO, the degradation of DDT was decreased and found to be 47.23 and 48.29 %. These results revealed that the $^{\bullet}OH$ and h^+ play a significant role in the DDT degradation under visible light. In addition, the formation $^{\bullet}OH$ under the irradiation of light was determined using DMPO supported ESR spectra and revealed that no ESR signals were observed under dark. While after the irritation in visible light 4 signals was observed and their intensity was increased with increasing the irradiation time 10 min [10]. Photo-catalytic degradation mechanism is given in supplementary information and the formation of the intermediates are illustrated in supporting Figure SF-3 and supported with reactive sites calculated with DFT calculation. The proposed schematic band structure and charge-transfer process of the $SrTiO_3/Ag_2O$(10)-NDC nanocomposite is displayed in Fig. 3(f).

4. Conclusion

In the present study, we have fabricated $SrTiO_3/Ag_2O$-NDC nanocomposite, it was noticed that Ag_2O tuned the bandgap and increased the adsorption of a wide range of solar energy, while the NDC adsorbed the DDT and increased the charge transfer process. The Ag_2O also acts as an electron trapping agent to decrease the charged electron and hole recombination. The fabricated nanocomposites show excellent catalytic activity and reusability for the degradation of DDT in contaminated water.

CRediT authorship contribution statement

Norah Alhokbany: Methodology, Formal analysis, Resources. **Tansir Ahamad:** Conceptualization, Methodology, Investigation, Writing – original draft. **Jahangeer Ahmed:** Visualization, Writing – review & editing. **Saad M Alshehri:** Funding acquisition, Resources, Supervision.

Declaration of Competing Interest

The authors declare that they have no known competing financial interests or personal relationships that could have appeared to influence the work reported in this paper.

Acknowledgment

The authors thank to Researchers Supporting Project number (RSP-2021/29), King Saud University, Riyadh, Saudi Arabia.

Appendix A. Supplementary data

Supplementary data to this article can be found online at https://doi.org/10.1016/j.matlet.2022.132271.

References

[1] B. Yu, J. Zeng, L. Gong, M. Zhang, L. Zhang, X. Chen, Investigation of the photocatalytic degradation of organochlorine pesticides on a nano-TiO2 coated film, Talanta 72 (5) (2007) 1667–1674.
[2] P. Debabrata, M. Sivakumar, Sonochemical degradation of endocrine-disrupting organochlorine pesticide Dicofol: investigations on the transformation pathways of dechlorination and the influencing operating parameters, Chemosphere 204 (2018) 101–108.
[3] J. Dang, S. Tian, Q. Zhang, Mechanism and kinetics studies of the atmospheric oxidation of p, p'-Dicofol by OH and NO3 radicals, Chemosphere 219 (2019) 645–654.
[4] D. Panda, S. Manickam, Hydrodynamic cavitation assisted degradation of persistent endocrine-disrupting organochlorine pesticide Dicofol: Optimization of operating parameters and investigations on the mechanism of intensification, Ultrasonics Sonochem. 51 (2019) 526–532.
[5] P. Ye, W. Xin, L. Zheng, Y.-H. Xie, Uniform growth of high-concentration MoS2 nanoflakes on plasma treated carbon nanotube sheet, Mater. Lett. 256 (2019).
[6] Z. He, J. Su, R. Chen, B. Tang, Fabrication of novel p-Ag2O/n-PbBiO2Br heterojunction photocatalysts with enhanced photocatalytic performance under visible-light irradiation, J. Mater. Sci.: Mater. Electron. 30 (23) (2019) 20870–20880.
[7] A.M. Al-Enizi, M. Naushad, A.a.H. Al-Muhtaseb, S.M. Ruksana, Z.A. Alshehri, T Ahamad Alothman, Synthesis and characterization of highly selective and sensitive Sn/SnO2/N-doped carbon nanocomposite (Sn/SnO2@NGC) for sensing toxic NH3 gas, Chem. Eng. J. 345 (2018) 58–66.
[8] T. Ahamad, M. Naushad, Ruksana, A.N. Alhabarah, S.M. Alshehri, N/S doped highly porous magnetic carbon aerogel derived from sugarcane bagasse cellulose for the removal of bisphenol-A, Int. J. Biol. Macromol. 132 (2019) 1031–1038.
[9] A.A. Al-Kahtani, S.M. Alshehri, M. Naushad, Ruksana, T. Ahamad, Fabrication of highly porous N/S doped carbon embedded with ZnS as highly efficient photocatalyst for degradation of bisphenol, Int. J. Biol. Macromol. 121 (2019) 415–423.
[10] W. Zhao, Y. Feng, H. Huang, P. Zhou, J. Li, L. Zhang, B. Dai, J. Xu, F. Zhu, N. Sheng, D.Y.C. Leung, A novel Z-scheme Ag3VO4/BiVO4 heterojunction photocatalyst: study on the excellent photocatalytic performance and photocatalytic mechanism, Appl. Catal. B: Environ. 245 (2019) 448–458.